

Performance inspection of high gain chopper designed to extract optimum output of photovoltaic source

Khadiza Akter¹, S. M. A. Motakabber¹, A. H. M. Zahirul Alam¹, Siti Hajar Yusoff¹, SajibAhmed²,
Tania Annur³

¹Department of Electrical and Computer Engineering, Kulliyyah of Engineering, International Islamic University Malaysia, Kuala Lumpur, Malaysia

²Department of Electrical and Electronic Engineering, University of Malaya, Kuala Lumpur, Malaysia

³Department of Computer Science and Engineering, Shanto Mariam University of Creative Technology, Dhaka, Bangladesh

Article Info

Article history:

Received Jan 29, 2023

Revised Apr 15, 2023

Accepted May 3, 2023

Keywords:

Continuous conduction mode

High gain chopper

MPPT

Quadratic cell

VDC

ABSTRACT

In recent years, the demand for power consumption has increased rapidly to fulfill the energy needs of households and industries worldwide. Solar electricity has emerged as the most practical form of renewable energy in this context. Due to its distinctive qualities such as being clean, quiet, and sustainable. Here, the study and analysis of a non-isolated high-gain chopper for solar photovoltaic (PV) systems are presented, which includes a quadratic cell and voltage doubler circuit (VDC). To ensure the utmost power produced by the solar system, the perturb and observe (P&O)-based maximum power point tracking (MPPT) algorithm is utilized. A quadratic VDC and a DC-DC boost converter are used to raise the PV voltage to a higher level (3.6 times higher with an MPPT controller, and 8 times higher with a battery source). The proposed converter exhibits notable improvements in efficiency, achieving an impressive 94%, which outperforms other state-of-the-art topologies. Additionally, the converter showcases a significant boost in voltage conversion gain, thereby substantiating its efficacy and superiority over other advanced topologies. Furthermore, comparatively less voltage stress on the switch with reduced voltage and current fluctuation increased the conversion effectiveness of the proposed configuration. Performance verification of the proposed topology is obtained by employing PSIM and MATLAB/Simulink.

This is an open access article under the [CC BY-SA](#) license.



Corresponding Author:

Khadiza Akter

Department of Electrical and Computer Engineering, Kulliyyah of Engineering

International Islamic University Malaysia

Kuala Lumpur, Malaysia

Email: khadiza@iubat.edu

1. INTRODUCTION

The goal of creating a carbon-free nation by 2050 has been set by numerous nations around the world [1]. The pressing need to achieve a sustainable, eco-friendly environment demands a substantial reduction in the usage of non-renewable fossil fuels such as coal, gas, and oil. Hence a worldwide concern has emerged to replace traditional fossil fuel-driven power generation with alternative energy sources that are not reliant on these depleting resources. One possible solution is to use renewable energy sources (RESs), like solar photovoltaic (PV) systems and fuel cells (FC) that are good for the environment, are connected to the utility grid, and have power electronics devices built in [2]. Due to its numerous benefits, including ease of allocation, lack of noise,

longer life, lack of pollution, quick installation, and output power capability to meet the highest load requirements, photovoltaic (PV) power generation has grown in importance as a renewable energy source [3].

In practical photovoltaic (PV) systems, the load level and external factors such as temperature and solar radiation undergo continuous fluctuations effectively regulate the operating point and sustain the system at maximum power point (MPP), the adoption of a suitable control algorithm and a high-performance DC-DC converter is imperative. With the help of MPPT controllers, power converters are mostly used to adjust the output voltage according to the needs of the application. The researcher has recommended numerous algorithms for maximum power point tracking (MPPT) operation for ease of use [4], [5]. P&O, Incremental conductance (IC) algorithm are the most commonly used methods. The new strategy has gained popularity in recent years, and it is based on fuzzy logic control (FLC) [6]. MPPT research also uses other artificial intelligence techniques. Additionally, MPPT converters using a soft switching technique are suggested to increase overall system efficiency [7].

The choice of a suitable photovoltaic (PV) converter is contingent upon several factors, including cost, adaptability, efficiency, and energy flow. Increasing the duty cycle in typical DC-DC step-up converters reduces stability and makes the control system more complex. The SEPIC, Cuk, and buck-boost converters are examples of well-known converters that can step up and down the source voltage. However, the insufficient output voltage adjustability makes boost and buck converters undesirable. When recommending DC-DC converters, a variety of aspects can be taken into account, including expense, flexibility, input/output flow of energy, and the impact of PV arrays. The SEPIC uses a back to back capacitor to separate input from output and has a non-inverted output [8]. Owing to input switching, discontinuous input current results in increased power loss in the buck and buck-boost converters' performances. Although the boost converter typically outperforms the SEPIC in terms of efficiency, the voltage output is always greater than the input, making it difficult to extract the maximum amount of power. It is feasible for the output voltage to be higher or lower than the input voltage using Cuk and SEPIC converters [6], [8].

Several studies have been done on different converter schemes, which can be split into non-isolated and isolated configurations based on how they are coupled and used to get around the problems listed above [9]–[13]. To use renewable energy, dual inductor-configured Switch Inductor (SI)-designed elevated lift-up converters are proposed [14]. The utilization of linked inductors in existing topologies leads to low efficiency due to the high level of leakage in the inductance coils. In contrast, the proposed converter configurations are built upon a single inductor that can generate a high voltage gain (HVG) while simultaneously maintaining exceptional efficiency. Even if the majority of these designs achieve HVG, using a large component count raises the converters' operational cost and complexity. A feedforward boost converter based on SL-SC can achieve HVG with fewer components, however, it cannot exploit high efficiency [15]–[17]. Few computational kinds of research have been proposed, and there are few studies on MPPT quadratic boost converters [18], [19].

In light of the aforementioned drawbacks, this article proposes a study and theoretical analysis of a high-gain chopper with a quadratic VDC and a P&O-based MPPT controller. Ultra-high gain is achieved using only a single switch and dual inductors, where VDC is combined with a quadratic structure. High-gain configurations suggested in [20]–[28] employ dual switches and have a significantly lower voltage gain than the converter provided in this study. The proposed configuration outperforms conventional PV and a battery source. Utilization of an MPPT controller did not deteriorate circuit permanence; rather, it can effectively transmit energy at all levels of radiation.

This paper is organized into five distinct sections, each with relevant subsections. Sections 2 and 3 provide an extensive literature review and background of the research. Following this, section 4 presents an in-depth analysis of the circuit's performance, while section 5 focuses on the results obtained from the experimentation and analysis. Finally, section 6 concludes the paper by summarizing the key finding and offering concluding remarks.

2. DESCRIPTION OF THE MPPT CONTROLLER

Numerous environmental factors, such as arbitrary shading, pollution, and wind issues, have an impact on PV power's sporadic functionality. Sunlight intensity varies significantly depending on the location and time of day; this causes variations in the solar cell's solar temperature and radiation. The design of the inverter next to the system is impacted by temperature and total resistance. The performance of photovoltaic (PV) power is subjected to wide range of environmental factors, such as shading, pollution, and wide-related issues, The intensity of sunlight varies significantly based on the location and time of day, leading to fluctuations in solar cell temperature and radiation.

Solar incorporated converters are used to raise the panel's voltage to its peak level and supply all of the effective power needed to extract the possible maximum power from the photovoltaic panel at any given time. The MPPT analyses the solar panel's supply current and voltage and chooses the operating point to supply

the load with the most generated power. To increase PV efficiency, the MPPT must accurately follow the dynamic operating region where the wattage is at its peak. There are different ways to determine the PV's peak power. The complexity, speed, accuracy, affordability, and number of sensors needed for each of these systems vary. Among the above-mentioned MPPT algorithms, P&O provides significant benefits, and numerous research projects have adopted it. In P&O, the challenges are the fluctuation issue and tracing MPP in the rapidly changing climate. However, it is not impossible to identify the correct MPP during sudden climate changes [29]. The process obtains its input from the solar PV array's actual operational point (current I_{pv} and voltage V_{pv}). Modifying the operating point (I_{pv} , V_{pv}), which is known as the perturbation step, and then evaluating the fluctuation in power (ΔP), which is termed the observational step, are the two steps used to scan the P-V curve in order to get MPP. Figure 1 depicts the proposed circuit with an MPPT block, whereas Figure 2 displays the usual P&O system's flow diagram.

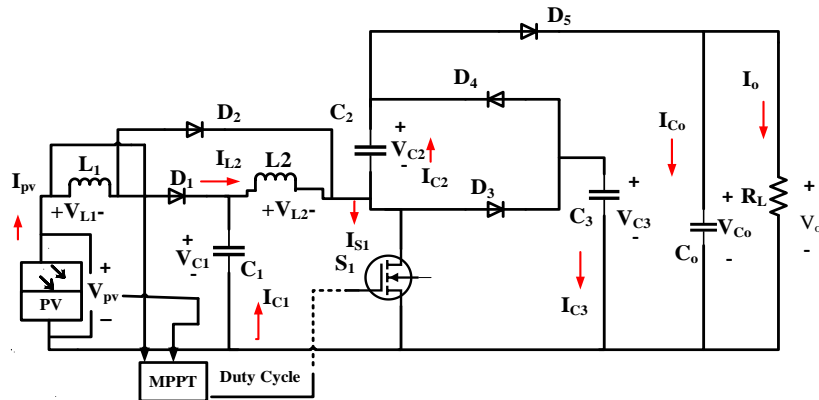


Figure 1. Proposed topology configuration along with MPPT controller

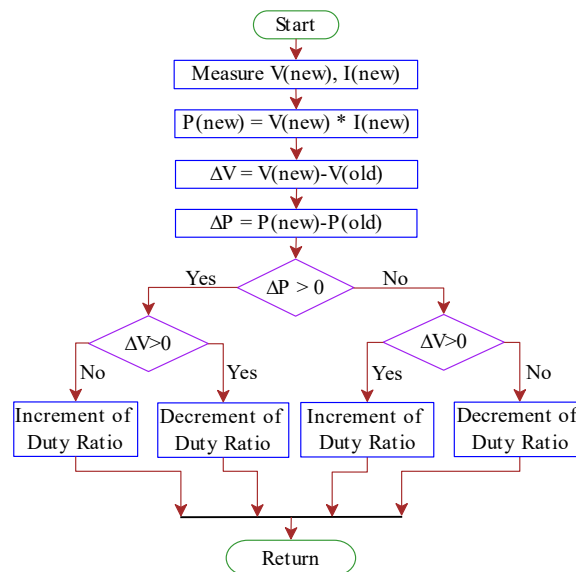


Figure 2. Block diagram of the conventional P&O MPPT algorithm

3. PROPOSED HIGH-PERFORMANCE CHOPPER

Figure 3 shows the suggested DC-DC converter structure. In the converter, there is only one switch (S), and it has two modes of operation displayed in Figures 4(a) and 4(b), respectively. The chopper circuit includes four capacitors, five diodes (D_1 , D_2 , D_3 , D_4 , and D_5), and two inductors (L_1 and L_2). Components L_1 , L_2 , C_1 , D_1 , and D_2 are performing a quadratic operation, whereas components C_2 , C_4 , D_3 , and D_4 are operating as a voltage doubler. The capacitor C_0 also discharges, and the energy it had stored is used to power the load. Figure 5 displays some significant waveforms for the power converters for both switching intervals.

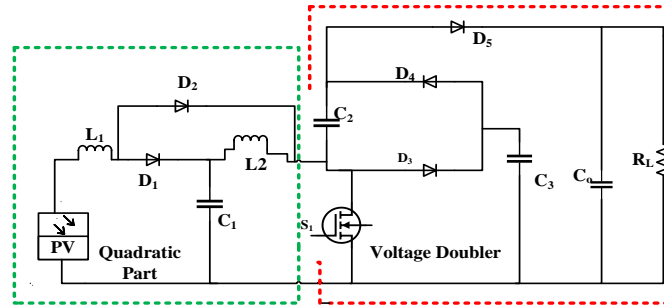


Figure 3. Equivalent circuit of the proposed chopper

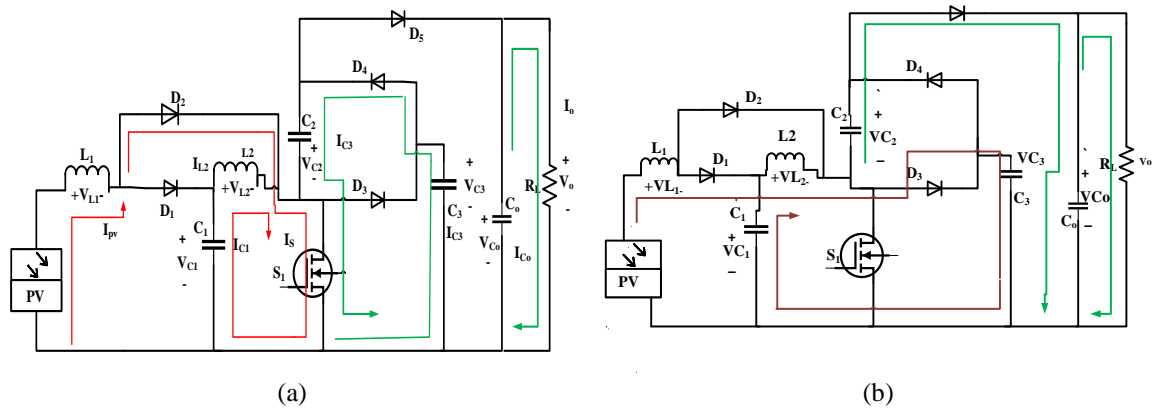


Figure 4. Equivalent circuit of the proposed configuration for (a) ON and (b) OFF period

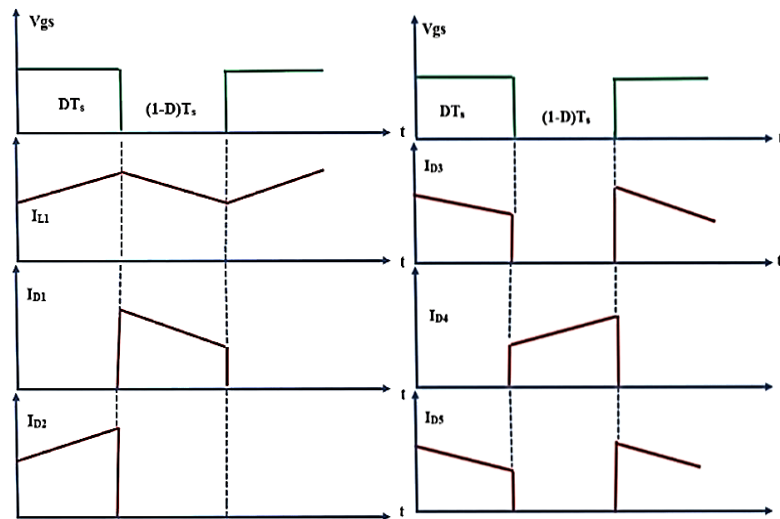


Figure 5. The theoretical waveform of the proposed converter

3.1. First operating mode ($0 < t < DT_s$)

Figure 4(a) depicts circuit operation mode I. The main switch has been switched on throughout this period, and diodes D_2 and D_4 are conducting. In this instance, current from the input supply flows through L_1 and D_2 . In this situation, inductor L_1 draws energy from the photovoltaic source, and inductor L_2 draws energy from C_1 . As a result, the currents flowing through inductors I_{L1} and I_{L2} grow linearly. Additionally, C_3 releases energy for charging C_2 . The capacitor C_0 also discharges, and the stored energy in it is used to power the load. The voltage across L_1 can be written as under:

$$\begin{aligned} V_{L1} &= L_1 \frac{dI_{L1}}{dt} = V_{in} \\ \frac{dI_{L1}}{dt} &= \frac{V_{in}}{L_1} DT \end{aligned} \quad (1)$$

where D stands for the duty cycle. Similarly, the voltage across L_2 can be written as under:

$$\begin{aligned} V_{L2} &= L_2 \frac{dI_{L2}}{dt} \\ \frac{dI_{L2}}{dt} &= \frac{V_{L2}}{L_2} \end{aligned}$$

For the switch ON condition, it can be written as (2).

$$\frac{dI_{L2}}{dt} = \frac{V_{L2}}{L_2} DT = \frac{V_{C1}}{L_2} DT \quad (2)$$

Similar to (1) and (2) for the OFF condition, changes in the current for inductors 1 and 2 can be written as (3) and (4).

$$\frac{dI_{L1}}{dt} = \frac{(V_{in} - V_{C1})}{L_1} (1 - D)T \quad (3)$$

$$\frac{dI_{L2}}{dt} = \frac{(V_{C1} - V_{C3})}{L_2} (1 - D)T \quad (4)$$

Applying KVL voltage across the capacitor is as (5).

$$\begin{cases} V_{C1} = V_{L2} \\ V_{C2} = V_{C0} - V_{C3} \\ V_{C0} = V_{C2} + V_{C3} \\ V_{C0} = V_o \end{cases} \quad (5)$$

Applying KCL, capacitor, diode, and inductor current relationship can be written as (6) and (7).

$$I_{PV} = I_{L1} = I_{D2} = I_S \quad (6)$$

$$\begin{cases} C_1 \frac{dV_{C1}}{dt} = I_{C1} = I_{L2} \\ C_2 \frac{dV_{C2}}{dt} = I_{C2} = I_{D4} \\ C_3 \frac{dV_{C3}}{dt} = I_{C3} = I_{D4} \\ C_o \frac{dV_{C0}}{dt} = I_{C0} = I_o \end{cases} \quad (7)$$

3.2. Second operating mode ($DT_S < t < T_S$)

The switch is not conducting at this time, causing the diodes D_1 , D_3 , and D_5 to be conductive while the other two are non-conductive. The equivalent circuit is depicted in Figure 4(b). Consequently, L_1 and L_2 function as a series-connected circuit. The energy that is stored in L_1 and L_2 is used to provide load support through C_2 and D_5 , as well as to charge C_1 and C_2 to transfer their energy. Applying KVL at the outer loop in Figure 4(b), potential difference across the inductor can be expressed as (8).

$$V_{L1} + V_{L2} = V_{in} - V_{C3} \quad (8)$$

Where in the inner loop it can be written as (9).

$$V_{L2} = V_{C1} - V_{C3} \quad (9)$$

The potential difference across the capacitor can be expressed as (10).

$$V_{C2} = V_{C0} = V_o \quad (10)$$

Applying KCL, capacitor, diode, and inductor current relationship can be written as (11).

$$\begin{cases} C_1 \frac{dV_{C1}}{dt} = I_{C1} = I_{L1} - I_{L2} \\ C_2 \frac{dV_{C2}}{dt} = I_{C2} = I_{L2} - I_{D3} \\ C_0 \frac{dV_{C0}}{dt} I_{C0} = I_{D5} - I_0 \end{cases} \quad (11)$$

3.3. Derivation of voltage gain

For inductive voltage volt second balance over one switching cycle is zero. Utilizing (4) and (6) equation it can be written as (12).

$$\begin{aligned} \int_0^{T_S} V_{L1}(t)dt &= 0 \\ V_{in}DT_S + (V_{in} - V_{C1})((1-D)T_S) &= 0 \\ V_{in}DT_S + (V_{in} - V_{C1})(T_S - DT_S) &= 0 \\ V_{in} - V_{C1} + DV_{C1} &= 0 \\ V_{in} &= V_{C1}(1-D) \\ \therefore V_{in} &= V_{C1}(1-D) \end{aligned} \quad (12)$$

From (2) and (4) volt second balance can be written as (13).

$$\begin{aligned} \int_0^{T_S} V_{L2}(t)dt &= 0 \\ V_{C1}DT_S + (V_{C1} - V_{C3})((1-D)T_S) &= 0 \\ V_{C1}DT_S + (V_{C1} - V_{C3})(T_S - DT_S) &= 0 \\ V_{C1}T_S - V_{C3}T_S(1-D) &= 0 \\ V_{C1}T_S &= V_{C3}T_S(1-D) \\ V_{C1} &= V_{C3}(1-D) \\ \therefore V_{C1} &= V_{C3}(1-D) \end{aligned} \quad (13)$$

Putting the value of V_{C1} in (12):

$$\begin{aligned} V_{in} &= V_{C1}(1-D) \\ V_{in} &= (1-D)V_{C3}(1-D) \\ V_{in} &= (1-D)^2V_0 \\ \frac{V_0}{V_{in}} &= \frac{1}{(1-D)^2} \end{aligned}$$

Using a voltage doubler circuit, the final equation will be (14).

$$\frac{V_0}{V_{in}} = 2 \frac{1}{(1-D)^2} \quad (14)$$

3.4. Equation of voltage stress on semiconductor components

Applying KVL, the voltage stress across the non-conducting element can be calculated. Hence the voltage between a switch and a diode, when they are not conducting, is given as (15).

$$\begin{aligned} V_{D1} &= V_{PV} \\ V_{Sw} &= V_{D3} = V_{D5} \\ V_{D4} &= V_{C2} \\ V_{D2} &= V_{L2} \\ V_{D5} &= V_{C0} \end{aligned} \quad (15)$$

3.5. Equitation of circuit parameters

Usually, the amount of ripple (between 5 and 10%) of the notional output current is taken into account to find the ideal size and loss for the converter.

$$L_1 = \frac{V_{PV}}{F_s \Delta I_{L1}} D \quad (16)$$

$$L_2 = \frac{V_{C1}}{F_S \Delta I_{L2}} D \quad (17)$$

Similarly, using the capacitor's rated voltage output as a starting point, a capacitor voltage fluctuation value of [5–10%] is assumed.

$$\Delta Q = \frac{I_0 D}{F_S} \quad (18)$$

$$\Delta V_C = \frac{\Delta Q}{C} \quad (19)$$

$$C = \frac{I_0 D}{\Delta V_C F_S} \quad (20)$$

4. RESULT AND DISCUSSION

4.1. Result analysis

To verify the theoretical findings, the design of the suggested converter circuit is developed and tested with MATLAB Simulink. The PV source used for simulation in MATLAB has a single parallel string and a single series-connected module per string. The values of the elements used for simulation are given in Table 1. Figures 6 show that the data used for simulation was a flawless convention for (a) PV source input and (b) converter output, producing the desired outcomes (V_{out} , I_{out} , and P_{out}) with a high level of efficiency.

Table 1. Parameters value chosen for simulation

Module type	AI green technology A10J-S72_175
Maximum Power	175 W
Cells per module	72
The voltage at the MPP	36.63 V
Current at the MPP	4.78 A
V_{OC}	43.99 V
I_{SC}	5.17 A
Solar irradiance	1000 W/m ²
Temperature	25 °C
Inductor L_1 , L_2	200 μ H
Capacitor C_1 , C_2 , C_3 , C_0	1000 μ F

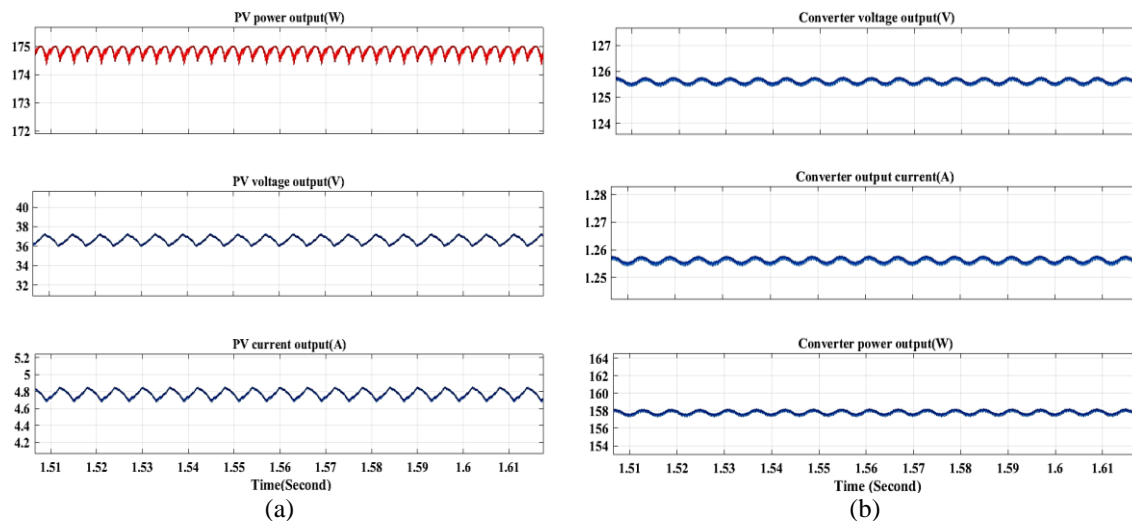


Figure 6. Power, voltage, and current output of (a) PV source and (b) converter of the proposed design

Figure 7 stated that, simulation and theoretical waveforms of the diodes current complies each other for D_1 , D_2 , D_3 and D_4 . Furthermore, Figure 8 illustrate the proposed DC-DC converter's simulation results for voltage across capacitors C_1 , and C_2 using the components and values listed in Table 1

for 36 V input. It is evident from the zoom view of the signal that the proposed circuit's simulation waveforms follow the theoretical waveform. To ensure more acceptability of the recommended circuit, the proposed design has been utilized with a battery source too. However, the inclusion of a battery source provides a more precise output which is displayed in Figure 9 in terms of input output voltage and current. The high fluctuation presents in inductor current and PV voltage in existing topology compares to the proposed topology is visible in Figure 10 to Figure 12 respectively.

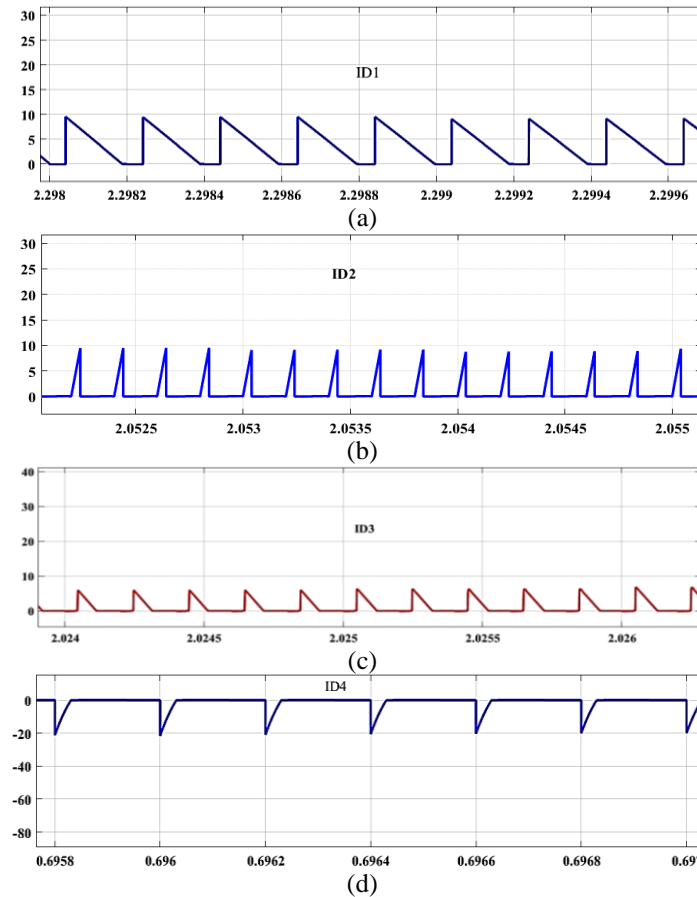


Figure 7. Waveshape of current carrying by diode (a) D_1 , (b) D_2 , (c) D_3 , and (d) D_4 the proposed topology

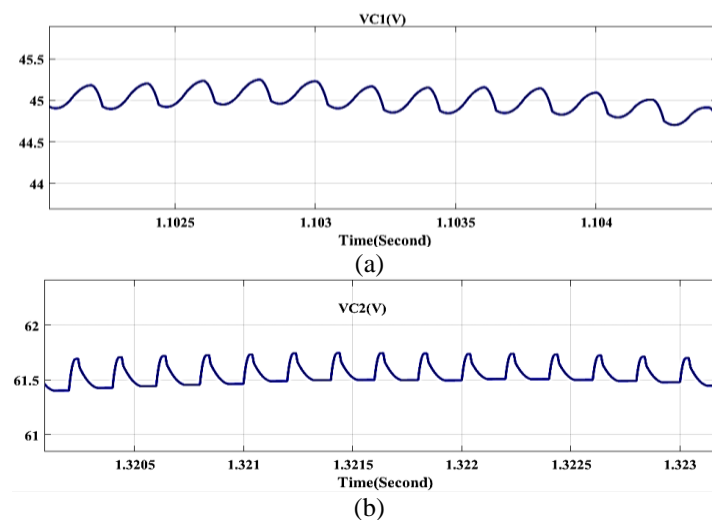


Figure 8. The waveform of voltage across the capacitor (a) C_1 and (b) (C_2) of the proposed topology

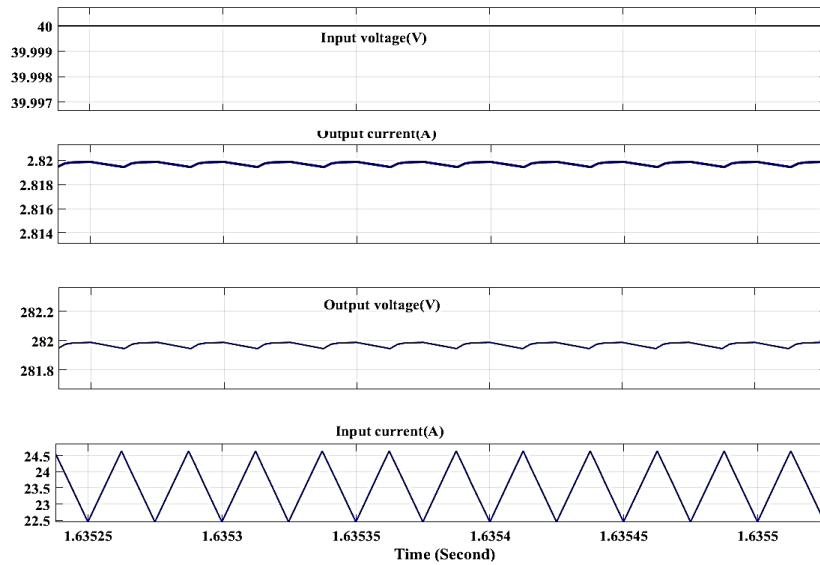


Figure 9. Input-output voltage and current of the proposed configuration with a battery source

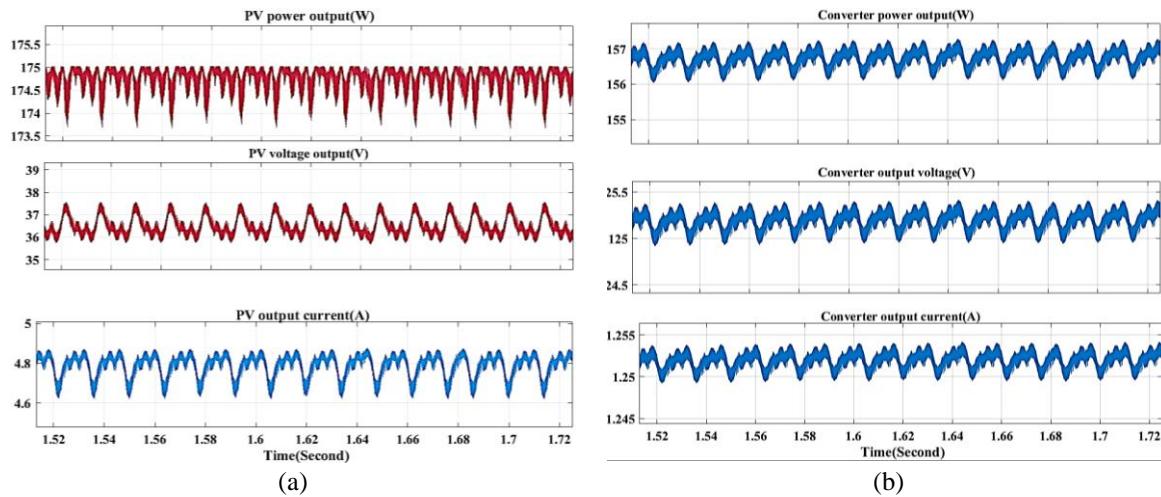


Figure 10. Power, voltage, and current output of (a) photovoltaic source and (b) SI converter [27]

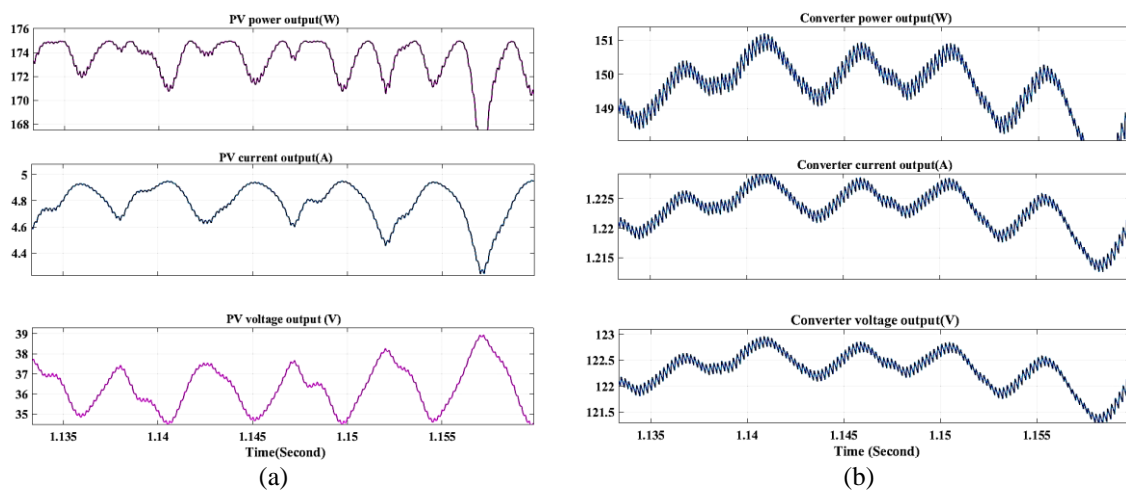


Figure 11. Power, voltage, and current output of (a) PV and (b) quadratic high gain cell converter [24]

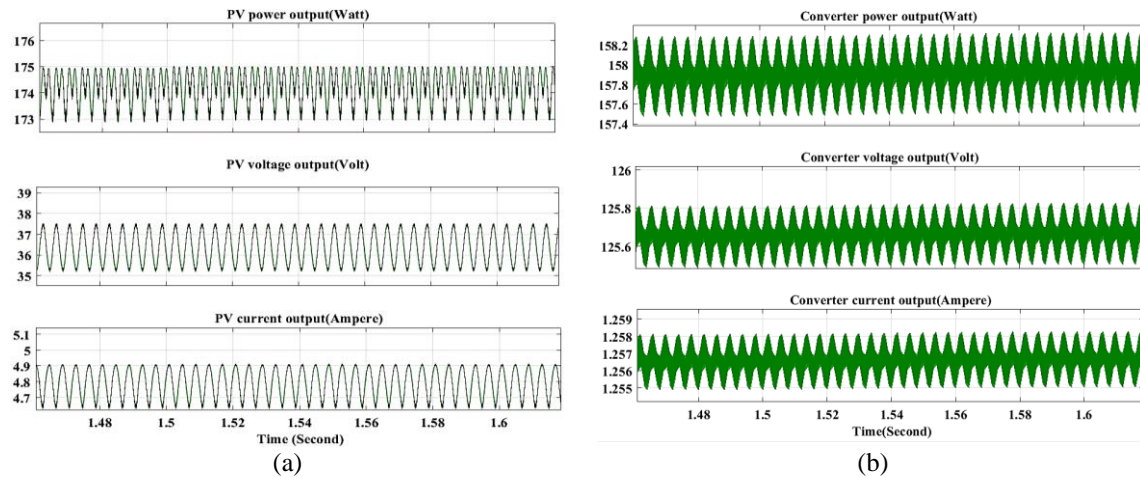


Figure 12. Power, voltage, and current output of (a) PV and (b) quadratic converter [28]

4.2. Comparative Analysis

In this study, a comparative analysis of the suggested converter and other existing technologies is performed based on key indicators, such as the number of inductors, capacitors, diodes, and switches, as well as the effectiveness of maximum power tracking. The results demonstrate the proposed topology has a distinct advantage in efficiently tracking maximum power, while other configurations struggle to meet this requirement. This observation is depicted in Figure 13. Additionally, Figures 14(a) and 14(b) presents a comparison of the voltage gain and conversion efficiency of the suggested topology with other designs. The supremacy of the proposed design with battery source in terms of efficiency and gain is shown in Figures 15(a) and 15(b) individually. Despite using fewer components than the suggested converter, the topology in [19] cannot achieve a significant voltage gain. A converter presented in [30] is exposed to extremely high voltage stress, including a poor voltage conversion ratio. The topologies suggested in [31], [32] can achieve a high gain in terms of voltage. Nevertheless, these topologies have required more components, and the switch is under severe voltage stress. In contrast to the suggested scheme, most topologies have reduced voltage gains and efficiencies for both PV and battery sources.

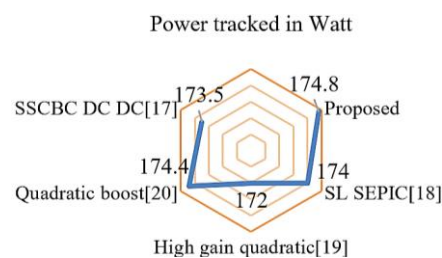


Figure 13. MPPT comparison of various topology

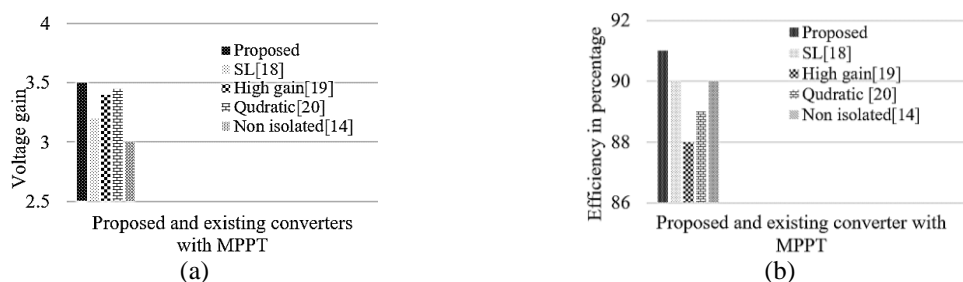


Figure 14. Efficiency comparison of existing and proposed converter in terms:
(a) voltage gain and (b) efficiency

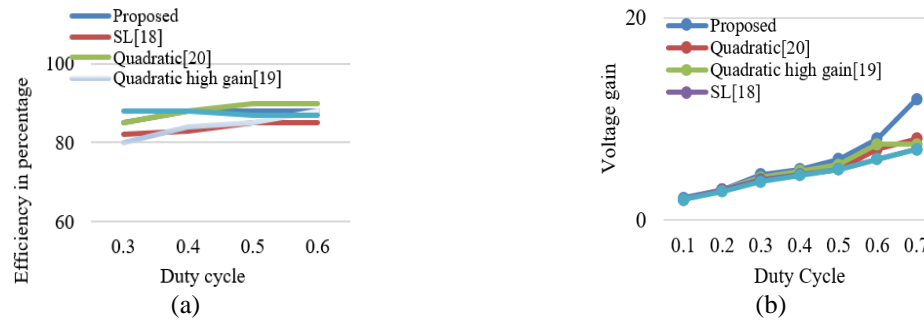


Figure 15. Performance comparison of various topology in terms of (a) efficiency and (b) voltage gain utilizing battery source

5. CONCLUSION

The present study details the design, development, and circuit analysis of a transformer less high step-up, non-isolated DC-DC chopper that is specifically tailored for solar photovoltaic (PV) systems. The proposed chopper is capable of achieving high gain using only a single switch and a quadratic cell-based VDC. At a duty ratio of 0.5, the voltage gain of the chopper is reported to be around eight times higher and even more at increased duty ratios when connected to a battery source, which is noticeably higher when compared to other converters. While incorporating a PV source, reduced fluctuation in current has been evaluated. Reduced voltage stress between capacitors influences the choice of low-power rating capacitors, increasing the converter's effectiveness (more than 90%) and reducing its cost. The proposed configuration is working efficiently for the PV and battery sources. Utilization of the P&O-based MPPT algorithm did not affect transformation efficiency; rather, other performance parameters improved significantly. Considering all these benefits, the proposed chopper can be implemented to step up the input voltage for applications requiring medium power.

ACKNOWLEDGEMENTS

The authors acknowledge the support from the International Islamic University Malaysia (IIUM) Engineering Merit Scholarship 2021.




REFERENCES

- [1] D. K. Panda and S. Das, "Smart grid architecture model for control, optimization and data analytics of future power networks with more renewable energy," *Journal of Cleaner Production*, vol. 301, 2021, doi: 10.1016/j.jclepro.2021.126877.
- [2] S. Ahmad, S. Mekhilef, and H. Mokhlis, "An improved power control strategy for grid-connected hybrid microgrid without park transformation and phase-locked loop system," *International Transactions on Electrical Energy Systems*, vol. 31, no. 7, 2021, doi: 10.1002/2050-7038.12922.
- [3] H. Chaieb and A. Sakly, "Comparison between P&O and P.S.O methods based MPPT algorithm for photovoltaic systems," *16th International Conference on Sciences and Techniques of Automatic Control and Computer Engineering, STA 2015*, pp. 694–699, 2016, doi: 10.1109/STA.2015.7505205.
- [4] Trishan and P. L. ChapmEsraman, "Comparison of photovoltaic array maximum power point tracking techniques," *IEEE Transactions on energy conversion*, vol. 22, no. 2, pp. 439–449, 2007.
- [5] B. T. Kadhem, S. S. Harden, and K. M. Abdulhassan, "High-performance Cuk converter with turn-on switching at zero voltage and zero current," *Bulletin of Electrical Engineering and Informatics*, vol. 12, no. 3, pp. 1359–1370, 2023, doi: 10.11591/eei.v12i3.4499.
- [6] A. El Khateb, N. A. Rahim, J. Selvaraj, and M. N. Uddin, "Fuzzy-logic-controller-based SEPIC converter for maximum power point tracking," *IEEE Transactions on Industry Applications*, vol. 50, no. 4, pp. 2349–2358, 2014, doi: 10.1109/TIA.2014.2298558.
- [7] S. Oncu and S. Nacar, "Soft switching maximum power point tracker with resonant switch in PV system," *International Journal of Hydrogen Energy*, vol. 41, no. 29, pp. 12477–12484, 2016, doi: 10.1016/j.ijhydene.2016.01.088.
- [8] K. M. Tsang and W. L. Chan, "Fast acting regenerative DC electronic load based on a SEPIC converter," *IEEE Transactions on Power Electronics*, vol. 27, no. 1, pp. 269–275, 2012, doi: 10.1109/TPEL.2011.2158446.
- [9] E. Sreelatha, A. Pandian, and M. S. Kuppasamy, "A novel topology for single-inductor single input triple output DC-DC power converter," *International Journal of Power Electronics and Drive Systems*, vol. 14, no. 1, pp. 304–310, 2023, doi: 10.11591/ijpeds.v14.i1.pp304-310.
- [10] K. Mahalingam and G. Jothamani, "An elevated gain DC-DC converter with active switched inductor for PV application," *International Journal of Power Electronics and Drive Systems*, vol. 14, no. 2, pp. 892–897, 2023, doi: 10.11591/ijpeds.v14.i2.pp892-897.
- [11] K. A. Mahafzah and H. A. Rababah, "A novel step-up/step-down DC-DC converter based on flyback and SEPIC topologies with improved voltage gain," *International Journal of Power Electronics and Drive Systems*, vol. 14, no. 2, pp. 898–908, 2023, doi: 10.11591/ijpeds.v14.i2.pp898-908.




- [12] S. Hasanzadeh, M. Asadi, and T. Sutikno, "Discontinuous conduction mode approach of ultra-lift DC-DC converter based on three windings coupled inductor," *International Journal of Power Electronics and Drive Systems*, vol. 14, no. 2, pp. 921–933, 2023, doi: 10.11591/ijpeds.v14.i2.pp921-933.
- [13] H. Al-Baidhani and A. Sahib, "Robust current-mode control of bridgeless single-switch SEPIC PFC converter," *International Journal of Power Electronics and Drive Systems*, vol. 14, no. 2, pp. 960–968, 2023, doi: 10.11591/ijpeds.v14.i2.pp960-968.
- [14] I. M. Pop-Calimanu, S. Lica, S. Popescu, D. Lascu, I. Lie, and R. Mirsu, "A new hybrid inductor-based boost DC-DC converter suitable for applications in photovoltaic systems," *Energies*, vol. 12, no. 2, 2019, doi: 10.3390/en12020252.
- [15] P. Sanjeevikumar, M. S. Bhaskar, P. Dhond, F. Blaabjerg, and M. Pecht, "Non-isolated sextuple output hybrid triad converter configurations for high step-up renewable energy applications," *Lecture Notes in Electrical Engineering*, vol. 436, pp. 1–12, 2017, doi: 10.1007/978-981-10-4394-9_1.
- [16] M. R. Banaei and S. G. Sani, "Analysis and Implementation of a New SEPIC-Based Single-Switch Buck-Boost DC-DC Converter with Continuous Input Current," *IEEE Transactions on Power Electronics*, vol. 33, no. 12, pp. 10317–10325, 2018, doi: 10.1109/TPEL.2018.2799876.
- [17] G. Zhang *et al.*, "An Impedance Network Boost Converter with a High-Voltage Gain," *IEEE Transactions on Power Electronics*, vol. 32, no. 9, pp. 6661–6665, 2017, doi: 10.1109/TPEL.2017.2673545.
- [18] T. Yan, J. Xu, Z. Dong, L. Shu, and P. Yang, "Quadratic boost PFC converter with fast dynamic response and low output voltage ripple," *2013 International Conference on Communications, Circuits and Systems, ICCAS 2013*, vol. 2, pp. 402–406, 2013, doi: 10.1109/ICCASCAS.2013.6765367.
- [19] N. Altin and E. Ozturk, "Maximum power point tracking quadratic boost converter for photovoltaic systems," *Proceedings of the 8th International Conference on Electronics, Computers and Artificial Intelligence, ECAI 2016*, no. June 2016, 2017, doi: 10.1109/ECAI.2016.7861151.
- [20] H. M. Maheri, E. Babaei, M. Sabahi, and S. H. Hosseini, "High Step-Up DC-DC Converter with Minimum Output Voltage Ripple," *IEEE Transactions on Industrial Electronics*, vol. 64, no. 5, pp. 3568–3575, 2017, doi: 10.1109/TIE.2017.2652395.
- [21] S. Gopinathan, V. S. Rao, and K. S., "Enhanced Voltage Gain Boost DC-DC Converter with Reduced Voltage Stress and Core Saturation," *IEEE Transactions on Circuits and Systems II: Express Briefs*, 2023, doi: 10.1109/TCSII.2023.3252721.
- [22] K. Akter, S. M. A. Motakabber, A. H. M. Z. Alam, and S. H. B. Yusoff, "Development of High-Performance Single Inductor Quadratic Multilevel DC-DC Step-Up Converter with MPPT Controller," *International Conference on Robotics, Electrical and Signal Processing Techniques*, vol. 2023-Janua, pp. 280–284, 2023, doi: 10.1109/ICREST57604.2023.10070035.
- [23] E. Oluwasogo, H. Cha, and T. Nguyen, "Beta-Quasi-Z-Source (β -qZS) DC-DC Converter Without Duty Cycle Constraint for Wide Input Voltage Applications," *IEEE Transactions on Industrial Electronics*, vol. 69, no. 12, pp. 12784–12794, 2022, doi: 10.1109/TIE.2021.3130324.
- [24] A. Kumar *et al.*, "A High voltage gain dc-dc converter with common grounding for fuel cell vehicle," *IEEE Transactions on Vehicular Technology*, vol. 69, no. 8, pp. 8290–8304, 2020, doi: 10.1109/TVT.2020.2994618.
- [25] T. Sutikno, H. S. Purnama, N. S. Widodo, S. Padmanaban, and M. R. Sahid, "A review on non-isolated low-power DC-DC converter topologies with high output gain for solar photovoltaic system applications," *Clean Energy*, vol. 6, no. 4, pp. 557–572, 2022, doi: 10.1093/ce/ztac037.
- [26] P. Rani L, S. Sekhar Dash, and R. K. Dwibedi, "Design and Implementation of Perturb Observe MPPT Algorithm under Partial Shading Conditions (PSC) for DC-DC Boost Converter by Simulation analysis," *International Conference on Computational Intelligence for Smart Power System and Sustainable Energy, CISPSSE 2020*, 2020, doi: 10.1109/CISPSSE49931.2020.9212221.
- [27] M. Y. A. Khan, H. Liu, S. Habib, D. Khan, and X. Yuan, "Design and Performance Evaluation of a Step-Up DC–DC Converter with Dual Loop Controllers for Two Stages Grid Connected PV Inverter," *Sustainability (Switzerland)*, vol. 14, no. 2, 2022, doi: 10.3390/su14020811.
- [28] S. Ozdemir, N. Altin, and I. Sefa, "Fuzzy logic based MPPT controller for high conversion ratio quadratic boost converter," *International Journal of Hydrogen Energy*, vol. 42, no. 28, pp. 17748–17759, 2017, doi: 10.1016/j.ijhydene.2017.02.191.
- [29] Y. Jiao, F. L. Luo, and M. Zhu, "Voltage-lift-type switched-inductor cells for enhancing DC-DC boost ability: Principles and integrations in Luo converter," *IET Power Electronics*, vol. 4, no. 1, pp. 131–142, 2011, doi: 10.1049/iet-pel.2010.0021.
- [30] Y. Almalaq and M. Matin, "Three topologies of a non-isolated high gain switched-inductor switched-capacitor step-up cuk converter for renewable energy applications," *Electronics (Switzerland)*, vol. 7, no. 6, 2018, doi: 10.3390/electronics7060094.
- [31] F. Sedaghati, M. E. Azizkandi, S. H. L. Majareh, and H. Shayeghi, "A High-Efficiency Non-Isolated High-Gain Interleaved DC-DC Converter with Reduced Voltage Stress on Devices," *2019 10th International Power Electronics, Drive Systems and Technologies Conference, PEDSTC 2019*, pp. 729–734, 2019, doi: 10.1109/PEDSTC.2019.8697263.
- [32] Y. Tang, D. Fu, T. Wang, and Z. Xu, "Hybrid switched-inductor converters for high step-up conversion," *IEEE Transactions on Industrial Electronics*, vol. 62, no. 3, pp. 1480–1490, 2015, doi: 10.1109/TIE.2014.2364797.

BIOGRAPHIES OF AUTHORS






Khadiza Akter    received an engineering degree in Electrical and Electronic Engineering from the International University of Business Agriculture Technology (IUBAT) of Bangladesh in 2011. She received her Master's degree in Power electronics from the Faculty of EEE from Islamic University of Technology (IUT) in 2018. She worked as an Assistant Professor at IUBAT from January 2019 to January 2022. Previously she served as a Lecturer at the same department from March 18, 2012 and subsequently promoted to Senior Lecturer and Assistant Professor. Currently, she is working as Research Assistant at the Laboratory of Power electronics and renewable energy research-Department of Electrical and Computer Engineering, International Islamic University Malaysia (IIUM). Her research interests include power electronics, renewable energy, and batteries. She can be contacted at email: khadiza@iubat.edu.






S. M. A. Motakabber    is an Associate Professor at the Department of Electrical and Computer Engineering, International Islamic University Malaysia, Malaysia, received the BSc (Honours) and Master's degrees from the University of Rajshahi in 1986 and 1987, and Ph. D from University Kebangsaan Malaysia in 2011. He served as a scientific officer at the Bangladesh Atomic Energy Commission, and Bangladesh Scientific and Industrial Research, Dhaka from 1991-1992 and 1992-1993, respectively. He started his teaching career as a lecturer in the Department of Applied Physics and Electronics, University of Rajshahi in 1993. The following year he was appointed an Assistant Professor in the same department. He joined as an Associate Professor in the Department of Computer and Communication Engineering at International Islamic University Chittagong in 2003; also served as Head of the Department and Dean of the Engineering Faculty. He can be contacted at email: amotakabber@iium.edu.my.






A. H. M. Zahirul Alam    received the B.Sc. and M.Sc. degrees in Electrical and Electronic Engineering from Bangladesh University of Engineering and Technology (BUET) in 1984 and 1987, respectively. He obtained his Doctor of Engineering degree from Kanazawa University, Japan in 1996. He was working as a faculty member in BUET from 1985 to 1991 and from 1996 to March 2002. He became a professor in BUET in 1999. He worked in the MIRAI project in Low-k group in Advanced Semiconductor Research Center, Tsukuba, Japan through Japan Science and Technology fellow from April 2002 to October 2003. He is currently serving as a Professor of Electrical and Computer Engineering Department, Faculty of Engineering, International Islamic University Malaysia (IIUM). His research interest includes electronic device modeling and fabrication, RF devices and MEMS, Energy harvesting system, antenna and communication devices. He can be contacted at email: zahirulalam@iium.edu.my.






Siti Hajar Yusoff    a former student of Kolej Yayasan UEM (KYUEM), Lembah Beringin. She obtained first class with honors in her MEng Degree (First Class Hons) (Electrical Engineering) and Doctor of Philosophy in Electrical & Electronic Engineering from the University of Nottingham, UK. Currently, she is attached to the Department of Electrical and Computer Engineering. Her specialization is in the area of power electronics and nonlinear control systems. Her research interests include wireless power transfer in electric vehicles (EV), energy management systems, renewable energy, microgrid, and IoT. She can be contacted at email: siti Yusoff@iium.edu.my.



Sajib Ahmed    received a B.Sc. degree in electrical and electronic engineering from the Chittagong University of Engineering and Technology (CUET), Bangladesh, in 2010. He is currently pursuing a master's in engineering from the Universiti Malaya, Malaysia in the department of electrical engineering. He has been associated with the Power Electronics and Renewable Energy Research Laboratory (PEARL), Universiti Malaya as a Graduate Research Assistant (GRA) since 2021. His research interests include renewable energy, solar-based dc-dc power converter topologies, maximum power point tracking, and energy efficiency. He can be contacted at email: s2034831@siswa.um.edu.my.



Tania Annur    received an engineering degree in Electrical and Electronic Engineering from the Ahsanullah University of Science and Technology (AUST) of Bangladesh in 2003, She received her Master's degree in Power electronics from the Faculty of EEE from Islamic University of Technology (IUT) in 2021. She worked as a Lecturer at Shanto Mariam University of Creative Technology (SMUCT), Bangladesh in CSE department from 2021 to till now. Previously she served as a Lecturer in City University, Bangladesh at EEE department from August 17, 2017. Her research interests include power electronics, renewable energy. She can be contacted at email: tania.annur1@gmail.com.